Assessment of Grid-Feeding Converter Voltage Stability

Junru Chen, *IEEE Student Member*, Federico Milano, *IEEE Fellow,* and Terence O'Donnell, *IEEE Member*

***Abstract*— This letter applies voltage stability analysis to grid feeding converters in the presence of the converter stability versus the grid state and its operation. By applying this analysis, it is shown that the converter may become unstable if the converter reference power or current exceeds the line capacity. The letter proposes to use a conventional PV curve to determine the stability of the dynamic response of grid-feeding converters considering both power and current limits.**

***Index Terms*— current limit, grid-feeding converter, reactive power compensation, stability criterion, voltage stability.**

I. Introduction

THe increase in renewable generation from solar plants and wind farms leads to an increase in power electronics converter interfaced sources in the grid. Presently, the majority of renewable sources are interfaced through 'grid-feeding' converters, i.e. converters that are controlled as current sources and impose the active power injection [1]. In this context, a stable operation of such grid feeding converter sources has a critical role in the system stability. Most of the previous work focuses on the internal stability of the converter, i.e. synchronization stability [2] and harmonic stability [3]. Faults also have a significant effect on the converter stability [4]. Due to the quick response of the converter (less than 10 ms), the fault can instantly drive the converter unstable. Thus, the ability of the control of the converters to maintain stability after the occurrence of a faults is critical to the overall grid stability.

Conventional voltage stability analysis is used to analyze the stability of the voltage at the load bus as a function of loading in steady state, under the assumption that the voltage at a generation bus is controlled and thus is given parameter in power flow analysis [5]. However, in grid-feeding converters, the converter voltage at the point of the common coupling (PCC) is not controlled directly and, thus, its value is obtained as a consequence of the control of the active power flow. An improper converter operation can lead to inappropriate voltage levels and, ultimately create the conditions for an unstable response of the converter. Therefore, in this letter, the voltage stability analysis is used to determine the impact on stability of the variations of voltage at converter buses rather than that at load buses.

Reference [6] is the first paper that applies such modified voltage stability analysis on the grid-feeding converter. However, [6] only considers the power capability limits of the converter. In this letter we show that, in practice, current limits of power electronic switches are the most binding. The main contribution of this work is, therefore, to study the grid-feeding converter voltage stability with inclusion of both power and current limits. The letter also shows, through detailed EMT real-time simulations, that steady-state PV curves define the stability of the dynamic response of the converters.

II. Grid-Feeding Converter

Grid-feeding converters, controlled as a current source, use a phase locked loop (PLL) to achieve synchronization at the PCC as shown in Fig. 1. The detected phase θ from the PLL tracks the PCC voltage phase δ. If synchronized, the q-axis PCC voltage in the synchronous dq-frame is 0 while d-axis PCC voltage e_d equals the voltage magnitude value $\sqrt{2}E$. In this case, the active and reactive power is decoupled and the current reference in dq-frame can be simply computed by the power reference over e_d. Therefore, as long as the PLL synchronizes, the power flow from the PCC to the grid can be controlled to the set point.

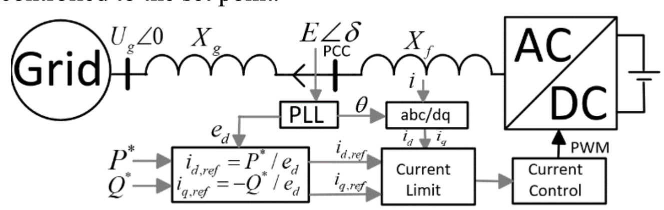

Fig. 1. Grid-Feeding Converter system structure (revise latter)

Assuming the grid voltage as the reference at 0 rad. The power flow from the grid-feeding converter to the grid is:

$$\text{P} = \frac{EU_g}{X_g}sin\delta, \quad \text{Q} = \frac{E^2}{X_g} - \frac{EU_g}{X_g}cos\delta \qquad (1)$$

where P/Q is active/reactive power, E is the RMS value of grid-feeding output voltage, U_g is the RMS value of grid voltage, X_g is the line impedance, and δ is the phase difference between two voltages.

In the grid-feeding converter, the delivered power P and Q is controlled to the reference values P^* and Q^* respectively. According to the grid voltage U_g and line impedance X_g, the grid-feeding converter output voltage $E\angle\delta$ is correspondingly changed to track the required reference power. Thus, the grid-feeding converter voltage is determined by the grid voltage, line impedance and power references. When the contingency occurs, e.g. grid voltage collapse (U_g reduces) or a line is lost (X_g increases), the deliverable power may fail to meet the required reference power. In this case, there is no operation point, and consequently the converter becomes unstable.

III. Converter Voltage Stability Assessment

The voltage stability analysis focuses on the converter voltage E associated with the renewable generation under the assumption that the grid voltage is the independent varying parameter. The analysis of the converter voltage stability uses the power-voltage (PV) curve. By eliminating δ in (1), the PV curve and VQ curve can be obtained as (2).

$$E = \sqrt{\frac{{U_g}^2}{2} + QX_g \pm \sqrt{\frac{{U_g}^4}{4} - P^2{X_g}^2 + QX_g{U_g}^2}} \quad (2)$$

Equation (2) gives the converter voltage required in order to deliver the active and reactive powers P, and Q to the grid through the impedance, X_g, assuming the grid voltage is U_g and this has the form of the blue line in fig. 2. The maximum deliverable power from the converter to the grid and its corresponding converter output voltage are:

$$P_{max} = \frac{1 + sin\varphi}{cos\varphi} \cdot \frac{{U_g}^2}{2X_g} \quad (4)$$

$$E_{Pmax} = \frac{U_g}{\sqrt{2}\sqrt{1 - sin\varphi}} \quad (5)$$

$$\varphi = \tan^{-1}\frac{Q}{P} \quad (6)$$

Obviously, the reactive power compensation can increase the maximum deliverable power and voltage stability. Note (E_{Pmax}, P_{max}) is the Saddle-node bifurcation point (SNB).

A. Reactive Power Compensation

Firstly, ignoring the converter current limit and assuming that the power to be delivered in (1) is the converter reference value $P*$, then the grid-feeding converter behaves like a constant power source as indicated by the solid black line in Fig. 2 (assuming $P^* = 1\,pu$). When the grid voltage reduces, the maximum deliverable power P_{max} from (4) reduces, and at some point, reduces below the reference power P^*, and unless $P*$ is also reduced, the converter becomes unstable.

In this case, the voltage to reactive power droop can be applied to increase the maximum deliverable power by compensating reactive power Q^*. The critical grid voltage where the converter becomes unstable for any P^*, Q^* combination can be derived as (7), which is computed by setting the maximum deliverable power in (4) equal to the reference power P^*.

$$U_{g,P} = \sqrt{\frac{2{P^*}^2X_g}{\sqrt{{P^*}^2 + {Q^*}^2} + Q^*}} \quad (7)$$

$U_{g,P}$ from (7) is the minimum grid voltage for which the converter could still output reference power stably. From this we can see that increasing Q^* and decreasing P^* makes $U_{g,P}$ smaller and increases the converter voltage stability.

B. Converter Capacity Limit

When the converter capacity S_{max} is considered, the reactive power compensation is limited by the active power.

$$Q^*_{max} = \sqrt{{S_{max}}^2 - {P^*}^2} \quad (8)$$

Substituting $P^* \in [0, S_{max}]$, and (8) into (2) could obtain the PV curve taking account of the converter capacity for any given grid voltage U_g. The solid blue line in Fig. 2 represents the converter PV curve where the grid voltage is at rated without any converter capacity limit, while the dashed blue line is the converter limited operating area assuming full excess capacity up to a limit of $S_{max} = 1.5\,pu$ is used for reactive power compensation.

C. Converter Current Limit

In practice, the converter capacity limit is further restricted by a current limit. When the reference current is saturated at its limit, the converter behaves like a constant current source as indicated by the dashed black line in Fig. 2 ($S_{max} = 1.5\,pu$), in which case the converter power is given by (9).

$$P = P_0\frac{E}{E_0} = I_{d,max}E, \quad Q = Q_0\frac{E}{E_0} = -I_{q,max}E \quad (9)$$

where P_0/Q_0 is the maximum active/reactive power at rated voltage E_0; $I_{d,max}/I_{q,max}$ is the active/reactive current limit set by the current limit in Fig. 1.

When the converter changes from the constant power source mode to constant current source mode, the grid voltage reduction leads to reduced converter output power, which benefits the converter voltage stability.

Substituting (9) into (2) gives the converter output voltage at the limited current as a function of the grid voltage.

$$E = -X_gI_{q,max} + \sqrt{{U_g}^2 - I^2_{d,max}{X_g}^2} \quad (10)$$

Essentially (10) gives the intersection point between the converter output power defined by (9) and the line capability curve defined by (2) and thus the PV operating point for the converter. For a valid operating point and stable operation, ${U_g}^2 \geq I^2_{d,max}{X_g}^2$. From (10), although $I_{q,max}$ could increase the converter output voltage, the stability is only related to $I_{d,max}$. The critical grid voltage is:

$$U_{g,I} = I_{d,max}X_g \quad (11)$$

Although at the critical voltage, the reactive power compensation $I_{q,max}$ could move the PV operating point in a range from (0,0) to $(-X_gI_{q,max}I_{d,max}, X_gI_{q,max})$, the critical grid voltage remains at $U_{g,I}$. If $I_{d,max}$, is reduced the converter voltage stability can be increased. Note, the operating point $(-X_gI_{q,max}I_{d,max}, X_gI_{q,max})$ is in the PV curve lower part, which is still stable as the phase remains locked by PLL.

IV. Validation Example

A 10 kV, 1.5 MW grid-feeding converter connected to a 50 Hz grid through a 50 mH transmission line is discussed in this section to illustrate the steady-state voltage stability analysis discussed in the previous section. A detailed real-time EMT simulation solved in Matlab/Simulink is used to validate the results obtained with the steady-state analysis. In the remainder of this section, the base voltage is 10 kV, the base power is 1 MW and the base impedance is 100 Ω. $S_{max} = 1.5\,pu$. The test examples include following cases:

- Case 1: No current limit, the converter works on constant power, $P^* = 1\,pu, Q^* = 0\,pu$
- Case 2: No current limit, the converter works on constant

power, $P^* = 1\,pu, Q^* = 0.1\,pu$.

● Case 3: With current limit, the converter works on constant current, $P^* = 1\,pu, Q^* = 0\,pu, I_{d,max} = 1.5\,pu$.

● Case 4: With current limit, the converter works on constant current, $P^* = 1\,pu, Q^* = 0.1\,pu$, $I_{d,max} = 1.5\,pu$, $I_{q,max} = -0.1\,pu$.

For the tests, the grid voltage drops from 1 *pu* to 0.57 *pu* and 0.56 *pu* at 1 s and 1.5 s respectively. The corresponding $U_{g,P} = 0.561\,pu$. The voltage then steps to 0.27 *pu* at 2 s. After that, it drops to 0.25 *pu*, 0.24 *pu* and 0.23 *pu* at 2.5 s, 3 s and 3.5 s respectively. For these voltages, the converter is current limited and the corresponding $U_{g,I} = 0.236\,pu$.

Figure 2 plots the PV curve results while Fig. 3 shows the converter active power output with time. At first, the operating point is at A in Fig. 2 corresponding to the solid blue curve when $U_g = 1\,pu$. If the converter continues working on constant power source mode (line AB1 in Fig. 2), when the grid voltage reduces to 0.57 *pu* at 1 s, due to $U_g > U_{g,P}$, the converter is still stable. When the grid voltage reduces further to 0.56 pu at 1.5 s, due to $U_g < U_{g,P}$, the converter without reactive power compensation (case 1) becomes unstable, which is the point B1 on the solid red line corresponding to $U_g = 0.56\,pu$, Q = 0 pu in Fig. 2. However, if 0.1 pu reactive power is compensated (case 2), the PV curve at $U_g = 0.56\,pu$ changes to the dash red line, then the converter is stable with the intersection point at B2. However, the stable margin in constant power mode is insufficient from Fig. 2, even though the reactive power compensated. Therefore, case 2 becomes unstable at 2 s when the grid voltage drops to 0.27 pu.

On the other hand, if the current limit is applied, after point X in Fig. 2, the converter works on the constant current source mode (line XO), $I_{d,max} = 1.5\,pu$. Thus, the power reduces when the grid voltage reduces to 0.57 pu. At 1.5 s, when the grid voltage drops to 0.56 pu, case 4 has slightly higher power output than case 3 since the operating point is at B3 but moves to B4 with reactive power compensation, $I_{q,max} = -0.1\,pu$. At 3 s, when the grid voltage drops to 0.24 pu, $U_g > U_{g,I}$, the converters for both case 3 and case 4 are stable, while the corresponding PV curves are the solid purple line and dash purple line in Fig. 2, where the operating points are C3 (0,0) and C4 (0.024, 0.016). However, at 3.5 s, when the grid voltage drops to 0.23 pu, $U_g < U_{g,I}$, the converters for both case 3 and case 4 become unstable, which verifies the point that although reactive power compensation can increase the deliverable power but it cannot improve the voltage stability.

V. Conclusions

This letter proposes a PV analysis to quantify the voltage stability of grid-feeding converters considering power and current limits and different control modes. The main conclusions are as follows: (i) in constant power source mode, from (7), the converter is stable if the grid voltage is greater than $U_{g,P}$; (ii) in constant current source operation, from (11), the converter is stable if the grid voltage is greater than $U_{g,I}$. In constant power source mode, the converter voltage stability can be enhanced through reactive power compensation, but this action has no influence on the constant current source mode voltage stability. However, decreasing the *d*-axis current limit can increase the converter voltage stability. With a flexible setting for the reference power in the constant power mode and the *d*-axis current limit in constant current mode, the grid-feeding converter can be made stable by imposing a maximum active power output during the fault. Future work will consider the stability of specific grid-feeding converter applications, i.e. wind farm, PV solar and HVDC links.

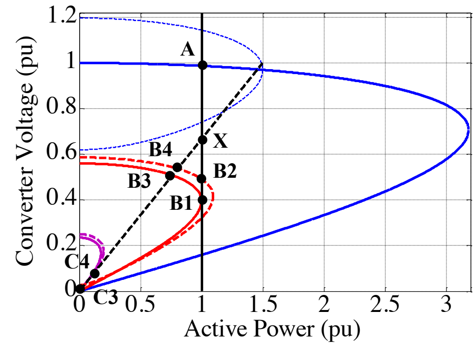

Fig. 2. PV Curve, solid blue line: $U_g = 1\,pu$, dash blue line: $U_g = 1\,pu, S_{max} = 1.5\,pu$, solid red line: $U_g = 0.56\,pu, Q^* = 0\,pu$, dash red line: $U_g = 0.56\,pu, Q^* = 0.1\,pu$, solid purple line: $U_g = 0.23\,pu, I_{q,max} = 0\,pu$; dash purple line: $U_g = 0.23\,pu, I_{q,max} = -0.1\,pu$, solid black line: constant power $P^* = 1\,pu$, dash black line: constant current $I_{d,max} = 1.5\,pu$

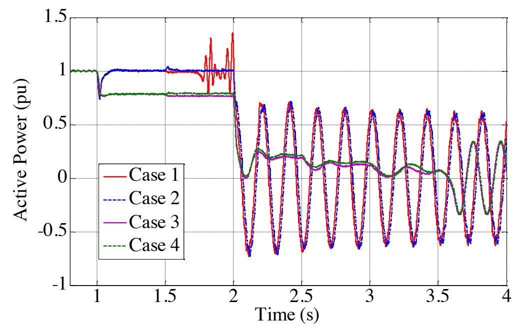

Fig. 3. Active power, t<1 s, $U_g = 1\,pu$, t=1~1.5 s, $U_g = 0.57\,pu$, t=1.5~2 s, $U_g = 0.56\,pu$, t=3~3.5 s, $U_g = 0.24\,pu$, t=3.5~4 s, $U_g = 0.23\,pu$,

References

[1] J. Rocabert, A. Luna, F. Blaabjerg and P. Rodríguez, "Control of Power Converters in AC Microgrids," in *IEEE Transactions on Power Electronics*, vol. 27, no. 11, pp. 4734-4749, Nov. 2012.

[2] M. G. Taul, X. Wang, P. Davari and F. Blaabjerg, "An Overview of Assessment Methods for Synchronization Stability of Grid-Connected Converters under Severe Symmetrical Grid Faults," *in IEEE Transactions on Power Electronics*, 2019.

[3] X. Wang, F. Blaabjerg and W. Wu, "Modeling and Analysis of Harmonic Stability in an AC Power-Electronics-Based Power System," in *IEEE Transactions on Power Electronics*, vol. 29, no. 12, pp. 6421-6432, Dec. 2014.

[4] M. Huang, Y. Peng, C. K. Tse, Y. Liu, J. Sun and X. Zha, "Bifurcation and Large-Signal Stability Analysis of Three-Phase Voltage Source Converter Under Grid Voltage Dips," in *IEEE Transactions on Power Electronics*, vol. 32, no. 11, pp. 8868-8879, Nov. 2017.

[5] T. Cutsem and C. Vournas, "Voltage Stability of Electric Power Systems," Kluwer Academic Publishers, Dordrecht, Netherlands, 01 Apr. 1998, ISBN10 0792381394.

[6] D. L. H. Aik and G. Andersson, "Fundamental Analysis of Voltage and Power Stability of Single-Infeed Voltage-Source Converter HVDC Systems," in *IEEE Transactions on Power Delivery*, vol. 34, no. 1, pp. 365-375, Feb. 2019.